Geophysical Research Letters

Correspondence to:
H. Liu,
liu.huixin.295@m.kyushu-u.ac.jp

Vertical Structure of Terdiurnal Tides in the Antarctic MLT Region: 15-Year Observation Over Syowa (69°S, 39°E)

Huixin Liu[1] ID**, Masaki Tsutsumi[2]** ID**, and Hanli Liu[3]** ID

[1]Department of Earth and Planetary Science, Kyushu University, Fukuoka, Japan, [2]National Institute of Polar Research, Tokyo, Japan, [3]National Center for Atmospheric Research, Boulder, CO, USA

Abstract The terdiurnal tide (TDT) in the Antarctic mesosphere and lower thermosphere region is poorly known. This study examines TDT using neutral wind observations at Syowa during years of 2004–2018. TDT is found to be a significant tidal component with distinct vertical structures and seasonal evolution. (1) It shows a prominent height-dependent seasonal variation with phase reversal at 94 km. (2) The vertical wavelength in summer is ∼40 km shorter than in winter. These features differ largely from those in the Arctic, indicating hemispheric asymmetry. The phase structure reveals a dominant upward propagating mode in local summer but superposition of more than one mode in other seasons. A downward propagating mode above 94 km in winter suggests Joule heating/ion drag as additional tidal sources to lower atmosphere ones. These results provide new constrains and benchmarks for model simulations that seek to understand terdiurnal tidal forcing mechanisms in polar regions.

Plain Language Summary Terdiurnal tides in the Antarctica mesosphere and lower thermosphere region are poorly known. In this study, we examine its characteristics using long-term neutral wind observations at Syowa (69°S, 39°E) between January 2004 and July 2018. The analysis reveals terdiurnal tide being a significant tidal component in the Antarctica around solstices with distinct vertical structures. (1) Tides above 94 km has opposite climatological variation to that below 94 km. (2) The zonal and meridional wind components are 90° phase shifted, with similar amplitude in most seasons. (3) The vertical wavelength is shorter in summer than in winter. Most of these features differ from those reported in the Arctic, indicating hemispheric asymmetry. Furthermore, the phase structure reveals a dominant upward propagating mode in local summer but superposition of more than one mode in other seasons. A downward propagating mode in winter above 95 km suggests Joule heating/ion drag as likely tidal sources from above, in addition to those from lower atmosphere. The nearly 15-year Syowa observations provide new constrains and benchmark for models that seek to understand terdiurnal tidal forcing mechanisms in polar regions.

1. Introduction

Atmospheric tides play an important role in the vertical coupling of the lower and upper atmosphere (e.g., Forbes, 1995). The terdiurnal tide (TDT) has been recognized in recently years to contribute significantly to the variability and dynamics of the mesosphere and lower thermosphere (MLT), with its amplitude approaching the dominant diurnal and semidiurnal tides in certain seasons (see, e.g., Du & Ward, 2010, and references therein). Characteristics of TDTs have been reported from a number of ground radar observations at low latitudes (Jiang et al., 2009; Rao et al., 2011), middle latitudes (e.g., Glass & Fellous, 1975; Jacobi, 2012; Teitelbaum et al., 1989; Thayaparan, 1997; Zhao et al., 2005), and also from satellite observations equatorward of 60°N/S (Moudden & Forbes, 2013; Smith, 2000; Yue et al., 2013). In contrast, TDT observations in polar regions (>60°N/S) fall short. Younger et al. (2002) reported TDT seasonal variation obtained from 1.5 years of wind observation at Esrange (68°N, 21°E). Oznovich et al. (1997) examined the TDT at Eureka (80°N) only in three short intervals (less than a month) in winter. TDTs in the Antarctica are yet to be revealed from observations.

On the other hand, the global structure of TDTs in the MLT region have been studied using various numerical simulations (Akmaev, 2001; Du & Ward, 2010; Smith & Ortland, 2001). Although their results are broadly
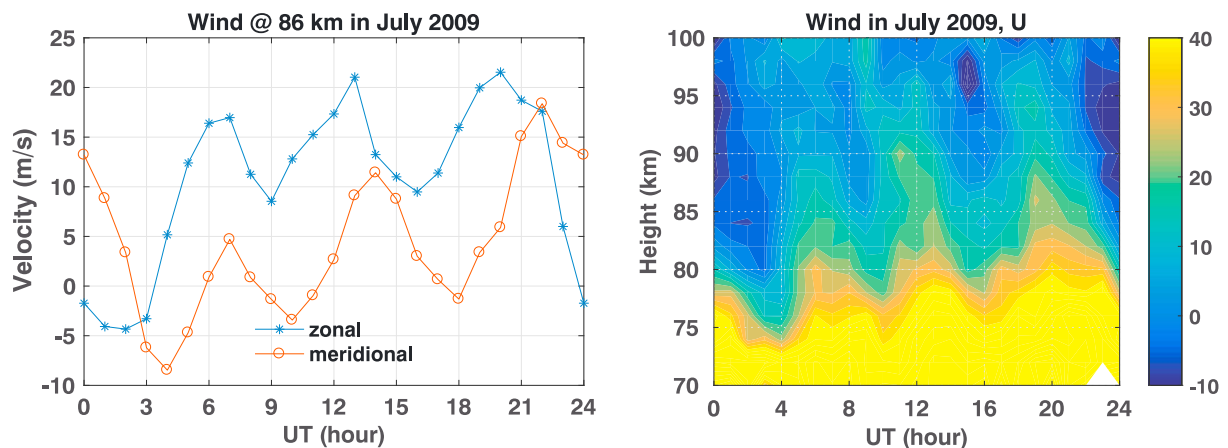
Figure 1. Average daily variation of wind in July 2009 at Syowa station (LT = UT + 2.6). (left) At 86-km height. (right) Height-UT cross section for zonal wind (meridional wind shows very similar feature). A prominent 8-hr period is visible in the wind.

consistent with observations in the Northern Hemisphere, intermodel discrepancies exist in the Southern Hemisphere where observations are lacking. For instance, the Spectral Mesosphere/Lower Thermosphere Model in Akmaev (2001) shows that the seasonal variation of TDT (in wind) in polar region at 94 km is semiannual, with larger amplitude in March than in January (see their Figure 2). In contrast, the primitive equation model (ROSE) in Smith and Ortland (2001) produced a seasonal variation in the opposite sense at 97 km, with peak TDT in June–July and minimum TDT around equinoxes (see their Figure 2). Using the Canadian Middle Atmosphere Model (CMAM), Du and Ward (2010) showed that TDT in wind at 95 km in southern polar region maximized in June–July and minimizes in December–January (see their Figure 3). These discrepancies demonstrate the deficiency in our understanding of wave sources and generation mechanism for TDTs in polar regions, and observations in the Antarctica are essential to clarify these discrepancies and make further progress. To provide this missing piece in the global picture, we examine the TDT using long-term wind observations from the Syowa medium-frequency (MF) radar in the Antarctica.

2. MF Radar System and Data Analysis Method

The Syowa MF radar is located at 69°S, 39°E. It is a monostatic pulse Doppler radar operating at 2.4 MHz with peak transmitting power of 50 kW. It has four antennas capable of both transmitting and receiving radio waves, which allow it to perform various interferometric observations. The antennas are located at the corners and the center of an equilateral triangle with side about 150 m long, with minimum antenna spacing of 0.7 λ (wavelength). This smaller distance than conventional MF radars (normally 1 λ) makes it possible to determine the echo arrival angles more accurately. Using full correlation analysis method, neutral wind velocity is derived from the radar observations at one hour cadence and 2-km height resolution between 66- and 100-km altitudes. Readers are referred to Tsutsumi and Aso (2005) for greater details on the radar facility and data processing.

This study employs neutral wind measurements between 1 January 2004 and 31 July 2018. Due to small signal-to-noise ratio at lower altitudes, we use only measurements between 75- and 100-km altitudes with measurement uncertainty below 0.1 m/s. Tidal components of 48, 24, 12, 8, and 6 hr are extracted from the wind data using a least squares fitting method with a 30-day window and 1-day shift (5-day shift produces slightly smaller amplitude but makes little difference in tidal features discussed below). Monthly mean tidal amplitude and phase are then obtained using vector averaging (Smith & Ortland, 2001) and are employed in the following analysis. Taking monthly mean helps to effectively remove signals with random or incoherent phases (e.g., gravity waves), which would be averaged out during 1-month period. We have repeated the analysis with 10- and 5-day windows and find no significant difference in the results described below. This robustness is likely owing to our taking monthly means.

3. Results
3.1. TDTs Over Syowa

Wind observations at Syowa sometimes exhibit quasi 8-hr periodicity, particularly prominent around solstices. An example is shown in Figure 1 for the average wind pattern in July 2009. Both the zonal and
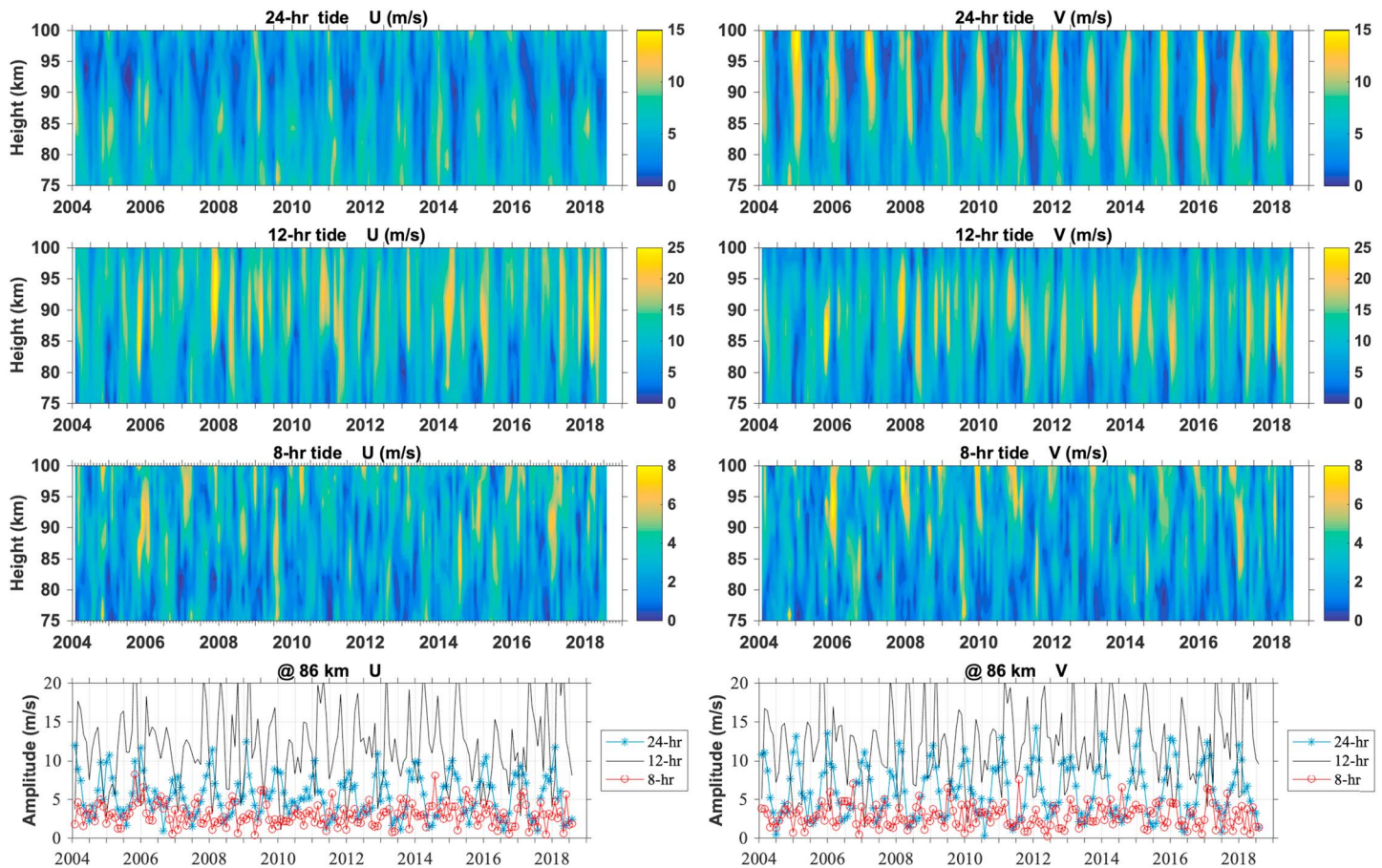
Figure 2. Amplitudes of different tidal components from January 2004 to July 2018. (left column) Zonal wind and (right column) meridional wind.

meridional wind components at 86-km altitude show three peaks during 24 hr (left panel), indicating the existence of significant terdiurnal tidal component. This signature exists at an extended altitude range of 75–100 km (right panel), with a downward phase propagation below 95 km.

Figure 2 shows the TDT in zonal (U) and meridional (V) wind during January 2004 to July 2018. Diurnal and semidiurnal tides are also shown for comparison. Although the TDT is overall much weaker, its monthly mean amplitude can reach 8 m/s and becomes comparable to semidiurnal and diurnal tides in solstice months as best seen in the bottom panels for tides at 86 km.

To uncover the dominant tidal features, we examine the monthly composite tides of the ~15-year observations using vector average. Note that by vector averaging over more than a solar cycle, interannual variability and variabilities with no coherent phases should all diminish. Consequently, the composite tides are highly free from contamination of gravity waves (e.g., Chen et al., 2016) and represent general features of dominant tidal components, which are more suitable to be compared to model predictions than short-term observations. The long-term averaging may also produce smaller tidal amplitude than those obtained during shorter period.

3.2. Seasonal Variation

Figure 3 shows the height-season structures of the composite tides in zonal (U) and meridional wind (V). The features are very smooth owing to the long-term average. The diurnal tide (top row) exhibits an annual variation with minimum in winter during May–July (season refers to local season unless otherwise mentioned), while the semidiurnal tides (panels in the second row) show the familiar semiannual variation with maxima around equinoxes. These seasonal variations persist throughout the altitude range of 75–100 km.

In contrast, the TDT (panels in the third row) shows a pronounced structure with two separate regions, where prominent peaks form around 86 km in winter (June–July), but above 94 km around November. This
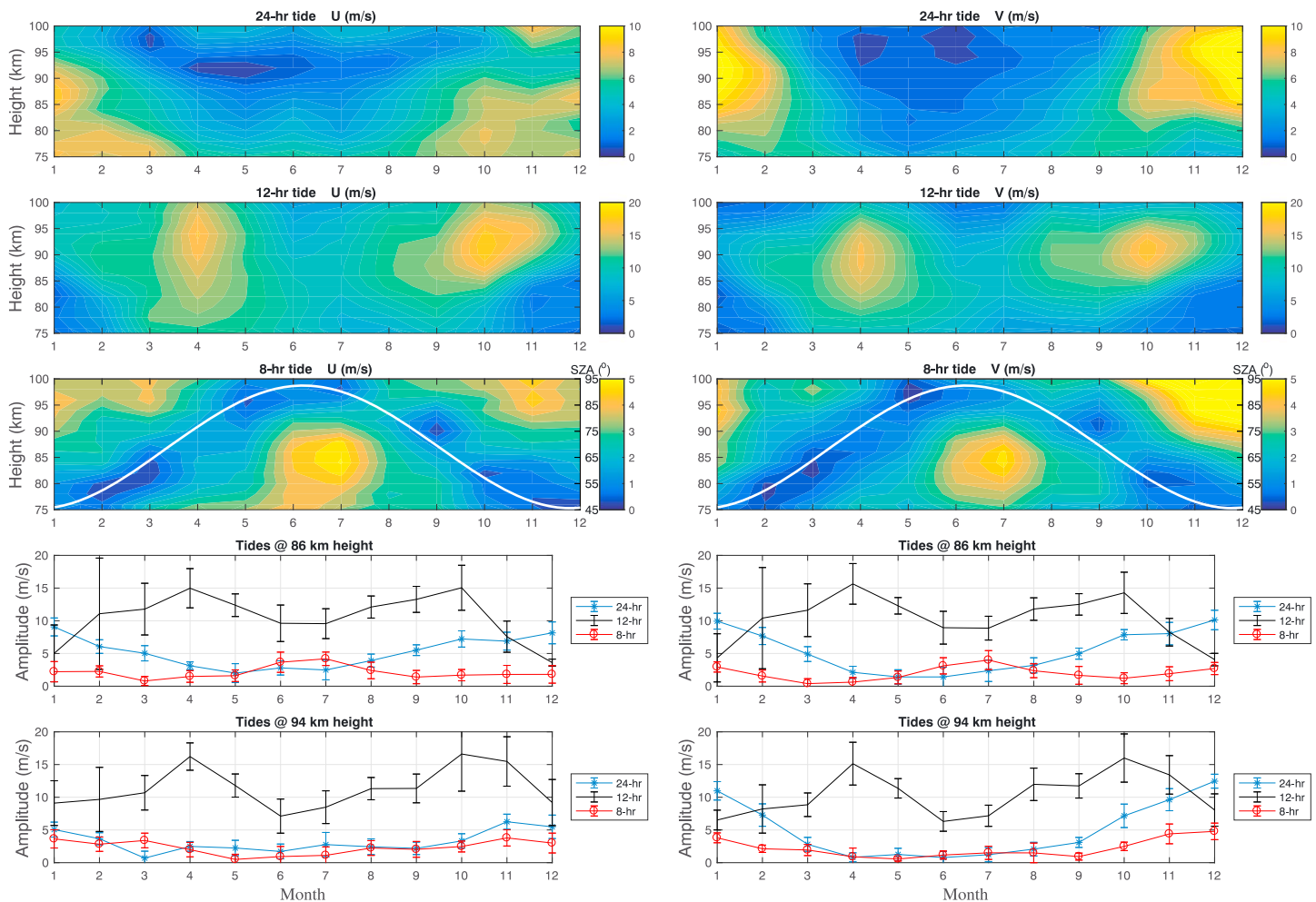
Figure 3. Amplitudes of composite tidal components calculated between January 2004 and July 2018. (left column) Zonal wind and (right) meridional wind. (top to bottom) Height versus month variation for the diurnal (24-hr) tide (first row), for the semidiurnal (12-hr) tides (second row), for the 8-hr tides (third row), tidal amplitudes at 86-km height (fourth row), and tidal amplitude at 94-km height (fifth row). The white line depicts the solar zenith angle at 12 LT noon, which exhibits similar seasonal trend to the height of minimum amplitude. Error bars indicate standard deviations.

distribution leads to a height-dependent seasonal variation unlike that of the diurnal and semidiurnal tides. For instance, the TDTs at ∼75 km shows annual variation with amplitude maximum in winter (June–July) and minimum in summer (December–January). Moving upward, two minima occur around equinoxes with the winter peak remaining. Above 94 km, the annual variation returns but in nearly opposite phase to that at 75 km with winter minimum and November maximum. These height-season structures appear consistently in both the zonal and meridional wind, implying that they are robust features of the TDT.

This height-dependent seasonal variation is very different from those observed in the Arctic in terms of local season. Using 1.5-year observations at Esrange (68°N, 21°E), Younger et al. (2002) found the TDT peaks in September to October at all altitudes between 80 and 98 km. However, all model simulations predict stronger TDTs in winter than in summer below 100 km (Akmaev, 2001; Du & Ward, 2010; Smith & Ortland, 2001), which is consistent with our observations below 94 km.

Line plots in the bottom panels of Figure 3 compare the terdiurnal amplitude with the diurnal and semidiurnal amplitudes at 86- and 94-km heights. The TDT exceeds the diurnal tide in winter (June–July) at 86 km, with composite amplitude of ∼5 m/s. In summer (December–January), it approaches the semidiurnal tides at both 86 and 94 km except for the zonal component at 94 km. Thus, the TDT is a significant tidal component in the MLT region around solstices.
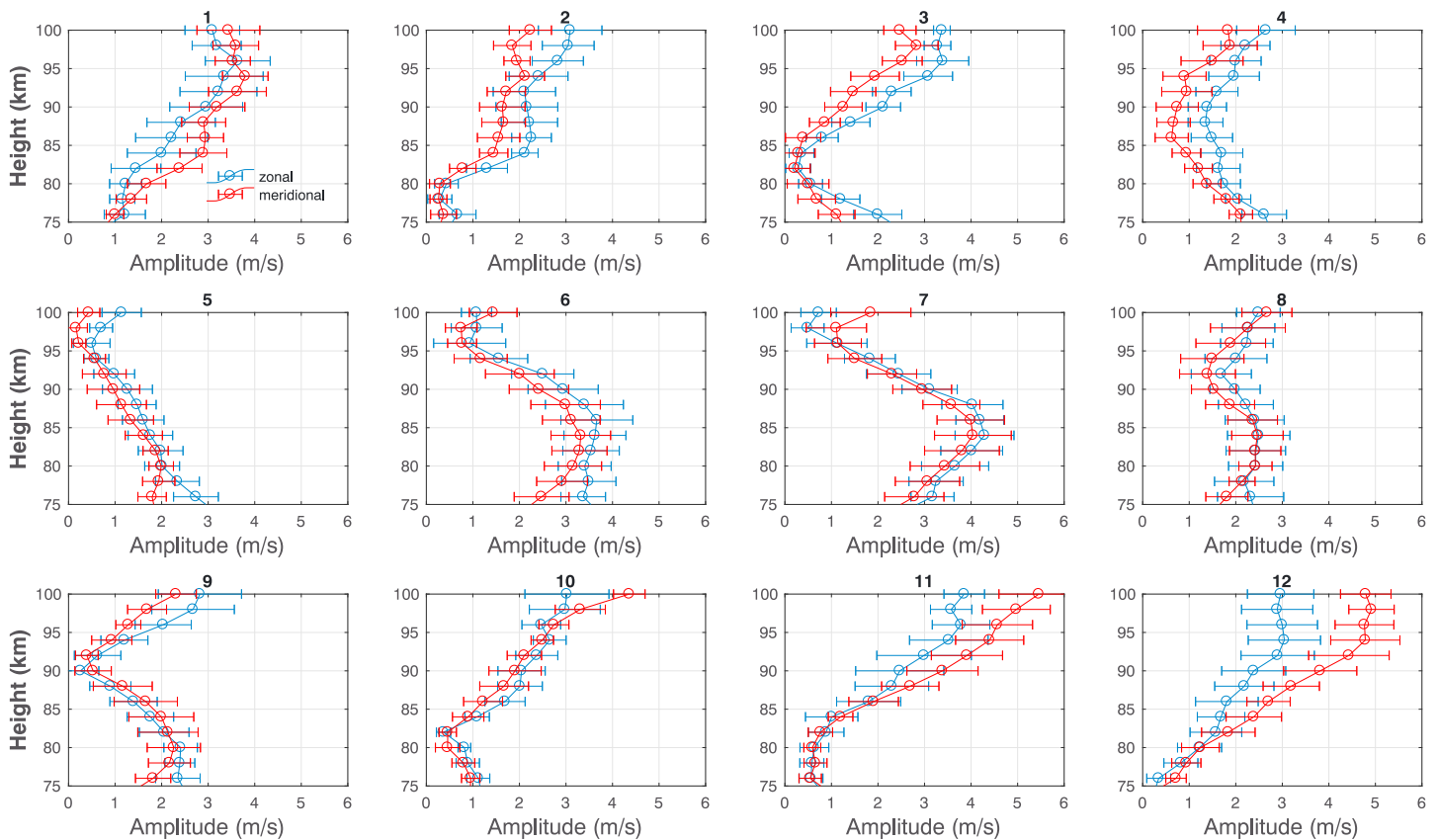
Figure 4. Height profiles of composite terdiurnal tidal amplitude in different months. The numbers 1–12 labeling each panel correspond to 12 months from January to December. Error bars indicate standard deviations. An amplitude minimum is clearly seen in the profiles during February–October, whose height shifts upward from March to July, then shits downward from July to October.

3.3. Vertical Structure of the TDT

The TDT shows distinct height dependence in its seasonal variation as described above. To provide further insight into the wave characteristics, we present the vertical profiles of the amplitude and phase in each month in Figures 4 and 5, respectively. In these figures, the numbers from 1 to 12 labeling each panel correspond to months from January to December. We see that the terdiurnal amplitude (Figure 4) in the zonal component (blue) is comparable to that of the meridional one (red) in all seasons except for summer (December–January). The phases (Figure 5) in two components are about 90° (2 hr) out of phase. Therefore, the TDT over Syowa appears to be circularly polarized, which is similar to those seen in the Arctic (Younger et al., 2002).

In summer (December–January), the amplitude increases roughly monotonically with altitude (Figure 4), which is accompanied by monotonic upward decrease in the phase. The phase profile is roughly linear, with a negative tilt angle throughout the altitude range of 75–100 km. This indicates a dominant upward propagating tidal mode with vertical wavelengths of about 50–60 km.

In other months (February–October), however, the linear feature gives way to a nonlinear one. The amplitude experiences decay and growth instead of a monotonic growth, with an amplitude minimum somewhere in the middle of the profile (e.g., at 82 km in March). The phase profile also becomes nonlinear, with a transition region of large phase shift that separates the profile into upper and lower parts (e.g., around 82–84 km in March in Figure 5). Note that the transition region well collocates with that of the minimum amplitude, which shifts upward from 78 km in February to 98 km in July then shifts downward again to 82 km in October. This seasonal shift follows the same trend of the noontime solar zenith angle (Figure 3, the white line in the third row). The nonlinear height variations in both amplitude and phase clearly indicate the presence of more than one tidal mode in the observational domain.
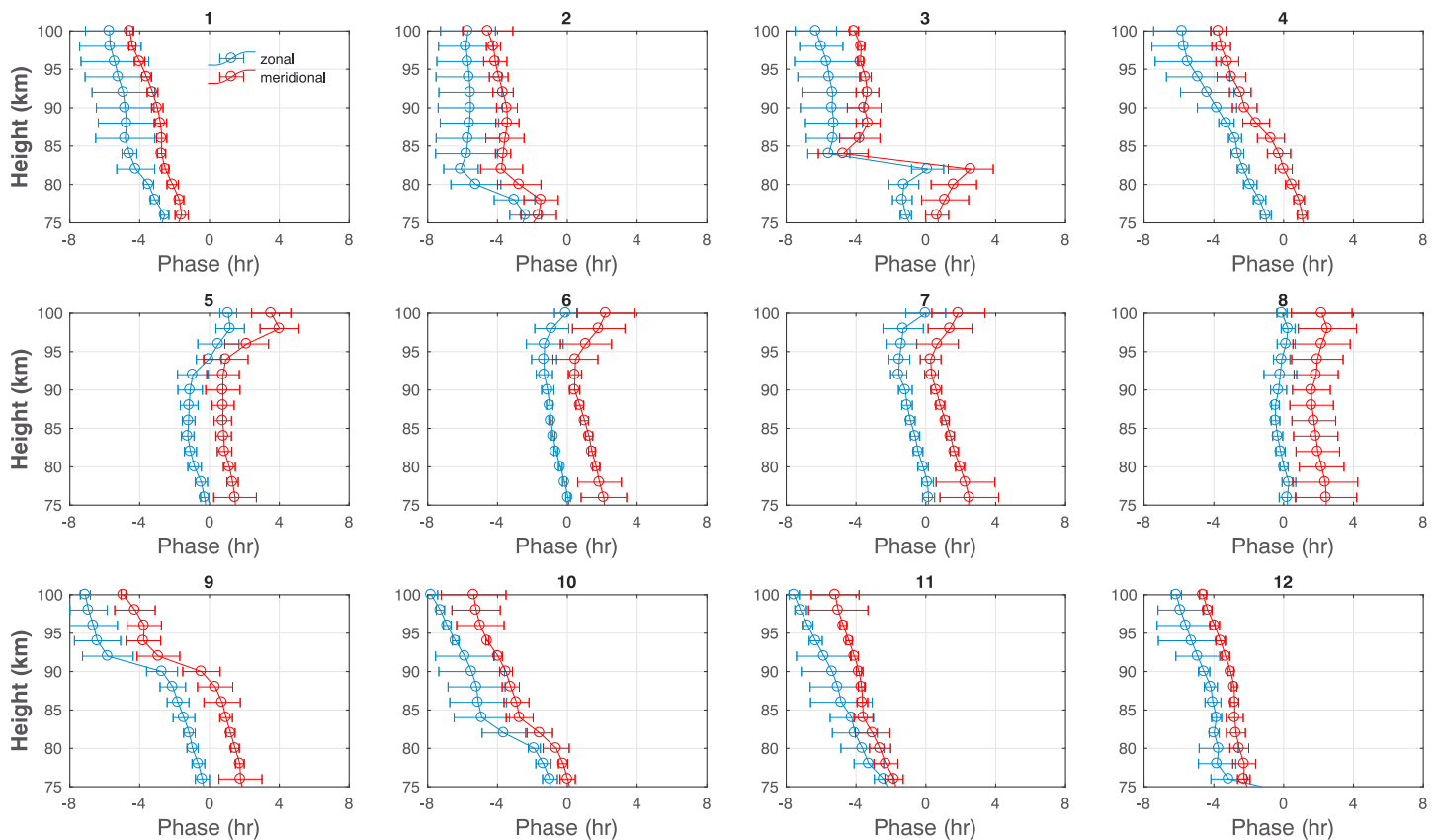
Figure 5. Same as Figure 4 but for phase. A transition region with large phase shift occurs in the profiles between February and October, whose height corresponds well to that of minimum amplitudes in Figure 4.

Particularly in winter (May–July), the transition region occurs high around 95 km (Figure 5). Above this height, the phase exhibits positive title angle, indicating a downward propagating mode. Below it, the phase profile shows a steep negative tilt, which yields a vertical wavelength of about 80–100 km. This nearly doubles the 50- to 60-km wavelength in summer (November–January). This seasonal variation is opposite to that in the Arctic reported by Younger et al. (2002), showing that the vertical wavelength is shortest in winter and spring (25–35 km) and longer in summer and autumn (50–90 km). But it agrees with simulation results of (Smith & Ortland, 2001) and is consistent with filtering effect due to background wind change with season, which is westward in summer and eastward in winter in southern polar region. The consistency between the zonal and meridional component in both the amplitude and phase lends to credibility of these features. Note that the vertical wavelength in winter is also much longer than the 20–30 km for gravity waves (Chen et al., 2016), providing addition evidence that these 8-hr waves are TDTs.

4. Discussion

The analysis of ~15-year wind observations at Syowa has revealed salient features in the TDTs in terms of seasonal variation and vertical structure. There are a few aspects that worth further discussion. Seasons below refer to local seasons unless otherwise mentioned.

First, its seasonal variation shows large difference from that at Esrange in the Arctic reported by Younger et al. (2002) in terms of amplitude and vertical wavelength as described in section 3. Differences in the utilized observation length (14.5 years at Syowa vs. 1.5 years at Esrange), and epoch (January 2004 to July 2018 at Syowa vs. October 1999 to April 2000) may contribute to some of these differences. But if we assume that the 1.5-year observation in Younger et al. (2002) can represent general features in the Arctic, these differences would reflect hemispheric asymmetry between the Arctic and Antarctica.

Second, its seasonal variation shows distinct height dependence, being in opposite phase above and below 94-km altitude (Figure 3, third row). Height-dependent seasonal variation in the Antarctica is predicted

by the CMAM (Du & Ward, 2010). This model predicts that the dominant terdiurnal component in the Antarctica is the migrating component, which peaks in winter (May–June) below 100 km but in summer (December–February) above it. Accounting for the 5-km uncertainty in geometric altitudes of the model (which is in pressure coordinate), these predictions are broadly consistent with our observations at Syowa. Furthermore, the observed phase variation also shows common features with the CMAM simulation (Figure 3 in Du & Ward, 2010), with fast phase transition around April–May and August–September. These consistency may suggest that the composite tides at Syowa obtained from long-term observations are likely dominated by migrating components. Observations in other longitude sectors are needed to ultimately verify this.

Third, the vertical structures of the TDT indicate a dominant upward propagating mode in summer but superposition of more than one mode in other seasons. The superposition produces a minimum in the amplitude, whose height shifts systematically with season (best seen in Figure 3 as the dark arc following the white line in the third row). What are the forcing mechanisms that causing these structures? Three generation sources for TDT have been proposed: solar heating of the stratospheric ozone (Chapman & Lindzen, 1970), nonlinear interaction between the diurnal and semidiurnal tides (Glass & Fellous, 1975; Teitelbaum et al., 1989), and interaction of the diurnal tide with gravity waves (Miyahara & Forbes, 1991). Among them, the latter two have been demonstrated to be significant only at low and middle latitudes (Akmaev, 2001; Du & Ward, 2010; Huang et al., 2007; Miyahara & Forbes, 1991; Smith & Ortland, 2001). At Syowa in the Antarctica, the lack of similarity between the seasonal variation of TDT and those of diurnal and semidiurnal tides also clearly indicates the negligible role of nonlinear interaction (e.g., TDT peaks in June–July when both diurnal and semidiurnal tides minimize in Figure 3). Thus, solar heating of the stratosphere ozone is left as the major wave source for TDTs at Syowa. This solar excitation from below along with background wind filtering effects seems to be consistent with the upward propagating mode in most months as indicated by the negative phase slopes. However, it cannot explain the unique tidal structure in winter (May–August), whose positive phase slope above 95 km indicates downward propagating wave at the topside.

What can drive a downward propagating wave? Local solar excitation above 100 km is unlikely due to lack of sunlight in polar winter. However, since Syowa (magnetic coordinates 70°S, 84°E) is located near the poleward edge of the auroral oval, it is not far fetched to speculate that Joule heating around 110–120 km or ion drag could be a source of excitation. Such an overhead source could produce downward propagating waves, though with decreasing amplitude due to the dense atmosphere below. None of the aforementioned model simulations produced the unique winter structure, which could be potentially due to the fact that none of them includes Joule heating/ion drag as an excitation source. On the other hand, one may ask why this downward propagating wave does not show up in other months? We currently do not have a clear explanation at our disposal, but it may have to do with the relative strength of the wave sources from above and below in different seasons. Numerical simulations with whole atmosphere models that include Joule heating/ion drag (e.g., WACCM-X model) could be carried out to examine these possibilities.

In summary, observations over more than one solar cycle at Syowa have revealed the TDT as a significant tidal component around solstices in the Antarctica. Its distinct vertical structure indicates that Joule heating and/or ion drag may need to be accounted for as an additional wave source by dynamical models that seek to understand forcing mechanisms of the TDT in polar regions. The long-term Syowa observations provide new constrains and benchmarks for future modeling efforts.

References

Akmaev, R. A. (2001). Seasonal variations of the terdiurnal tide in the mesosphere and lower thermosphere: A model study. *Geophysical Research Letters*, *28*, 3817–3820. https://doi.org/10.1029/2001GL013002

Chapman, S., & Lindzen, R. S. (1970). *Atmospheric tides: Thermal and gravitational*. Dordrecht, Netherland: D. Reidel Publishing Company.

Chen, C., Chu, X., Zhao, J., Roberts, B. R., Yu, Z., Fong, W., et al. (2016). Lidar observations of persistent gravity waves with periods of 3-10 h in the Antarctic middle and upper atmosphere at McMurdo (77.83°S, 166.67°E). *Journal of Geophysical Research: Space Physics*, *121*, 1483–1502. https://doi.org/10.1002/2015JA022127

Du, J., & Ward, W. E. (2010). Terdiurnal tide in the extended Canadian Middle Atmospheric Model (CMAM). *Journal of Geophysical Research*, *115*, D24106. https://doi.org/10.1029/2010JD014479

Forbes, J. (1995). Tidal and planetary waves. In R. M. Johnson & T. L. Killeen (Eds.), *Geophysical Monograph 87: The upper mesosphere and lower thermosphere* (pp. 67–87). Washington, DC: American Geophysical Union.

Glass, M., & Fellous, J. L. (1975). The eight-hourly (ter-diurnal) component of atmospheric tides. *Space Research*, *XV*, 191–197.

Huang, C. M., Zhang, S. D., & Yi, F. (2007). A numerical study of the impact of nonlinearity on the amplitude of the migrating diurnal tide. *Journal of Atmospheric and Solar-Terrestrial Physics*, *69*, 631–648. https://doi.org/10.1016/j.jastp.2006.10.008

Jacobi, C. (2012). 6 year mean prevailing winds and tides measured by VHF meteor radar over Collm (51.3°N, 13.0°E). *Journal of Atmospheric and Solar-Terrestrial Physics*, *78*, 8–18. https://doi.org/10.1016/j.jastp.2011.04.010

Jiang, J., Xu, J., & Franke, S. J. (2009). The 8-h tide in the mesosphere and lower thermosphere over Maui (20.75°N, 156.43°W). *Annals of Geophysics*, *27*, 1989–1999. Retrieved from https://www.ann-geophys.net/27/1989/2009/

Miyahara, S., & Forbes, J. (1991). Interaction between gravity waves and the diurnal tide in the mesosphere and lower thermosphere. *Journal of the Meteorological Society of Japan*, *69*, 523–531.

Moudden, Y., & Forbes, J. M. (2013). A decade-long climatology of terdiurnal tides using TIMED/SABER observations. *Journal of Geophysical Research: Space Physics*, *118*, 4534–4550. https://doi.org/10.1002/jgra.50273

Oznovich, I., McEwen, D. J., Sivjee, G. G., & Walterscheid, R. L. (1997). Tidal oscillations of the Arctic upper mesosphere and lower thermosphere in winter. *Journal of Geophysical Research*, *102*, 4511–4520. https://doi.org/10.1029/96JA03560

Rao, N. V., Tsuda, T., Gurubaran, S., Miyoshi, Y., & Fujiwara, H. (2011). On the occurrence and variability of the terdiurnal tide in the equatorial mesosphere and lower thermosphere and a comparison with the Kyushu-GCM. *Journal of Geophysical Research*, *116*, D02117. https://doi.org/10.1029/2010JD014529

Smith, A. K. (2000). Structure of the terdiurnal tide at 95 km. *Geophysical Research Letters*, *27*, 177–180. https://doi.org/10.1029/1999GL010843

Smith, A. K., & Ortland, D. A. (2001). Modelling and analysis of the structure and generation of the terdiurnal tide. *Journal of the Atmosphere Sciences*, *5*, 3116–3134.

Teitelbaum, H., Vial, F., Manson, A. H., Giraldez, R., & Massebeup, M. (1989). Non-linear interaction between the diurnal and semidiurnal tides: Terdiurnal and diurnal secondary waves. *Journal of Atmospheric and Terrestrial Physics*, *51*, 627–634.

Thayaparan, T. (1997). The terdiurnal tide in the mesosphere and lower thermosphere over London, Canada (43°N,81°W). *Journal of Geophysical Research*, *102*, 21,695–21,708.

Tsutsumi, M., & Aso, T. (2005). MF radar observations of meteors and meteor-derived winds at Syowa (69° S, 39°), Antarctica: A comparison with simultaneous spaced antenna winds. *Journal of Geophysical Research*, *110*, D24111. https://doi.org/10.1029/2005JD005849

Younger, P. T., Pancheva, D., Middleton, H. R., & Mitchell, N. J. (2002). The 8-hour tide in the Arctic mesosphere and lower thermosphere. *Journal of Geophysical Research*, *107*(A12), 1420. https://doi.org/10.1029/2001JA005086

Yue, J., Xu, J., Chang, L. C., Wu, Q., Liu, H.-L., Lu, X., & Russell, J. (2013). Global structure and seasonal variability of the migrating terdiurnal tide in the mesosphere and lower thermosphere. *Journal of Atmospheric and Solar-Terrestrial Physics*, *105*, 191–198. https://doi.org/10.1016/j.jastp.2013.10.010

Zhao, B., Wan, W., Liu, L., Yue, X., & Venkatraman, S. (2005). Statistical characteristics of the total ion density in the topside ionosphere during the period 1996–2004 using empirical orthogonal function (EOF) analysis. *Annales de Geophysique*, *23*, 3615–3631.